Cancer Cell International

RESEARCH

Open Access

Cancer-secreted exosomal miR-1825 induces angiogenesis to promote colorectal cancer metastasis

Jingbo Sun[1,2†], Junjie Luo[2†], Jialong Liu[2†], Hongmei Wu[1], Yanyan Li[1], Yangwei Xu[1], Lixin Liu[2*], Xiaolong Liu[2*] and Qingling Zhang[1*]

Abstract

Background Angiogenesis is one of the important factors related to tumorigenesis, invasion, and metastasis. Cancer-secreted exosomes are essential mediators of intercellular cross-talk and participate in angiogenesis and metastasis. Unveiling the mechanism of angiogenesis is an important way to develop anti-angiogenesis therapeutic strategies to against cancer progression.

Methods miR-1825 expression and relationship with microvascular density were validated in colorectal cancer (CRC) by in situ hybridization (ISH) staining and immunohistochemistry (IHC). Sequential differential centrifugation, transmission electron microscopy, and western blotting analysis were used to extract and characterize exosomes. The effort of exosomal miR-1825 on endothelial cells was examined by transwell assay, wound healing assay, tube formation assay, and aortic ring assay. The relationship of miR-1825, ING1 and the downstream pathway were analyzed by western blot, RT-PCR, Immunofluorescence, and dual-luciferase reporter system analysis.

Results Exosomal miR-1825 is associated with angiogenesis in CRC and is enriched in exosomes extracted from the serum of CRC patients. The CRC-secreted exosomal miR-1825 can be transferred into vascular endothelial cells, promoting endothelial cell migration and tube formation in vitro, and facilitating angiogenesis and tumor metastasis in vivo. Mechanistically, exosomal miR-1825 regulates angiogenesis and tumor metastasis by suppressing inhibitor of growth family member 1 (ING1) and activating the TGF-β/Smad2/Smad3 signaling pathway in the recipient HUVECs.

Conclusions Our study demonstrated the CRC-secreted exosomal miR-1825 could be transferred to vascular endothelial cells, subsequently leads to the inhibition of ING1 and the activation of the TGF-β/Smad2/Smad3 signaling pathway, thereby promoting angiogenesis and liver metastasis in CRC. Exosomal miR-1825 is thus a potential diagnostic and therapeutic target for CRC patients.

Keywords Angiogenesis, Exosomes, Colorectal cancer, miR-1825, ING1

† Jingbo Sun, Junjie Luo, and Jialong Liu have contributed equally to this work.

*Correspondence:
Lixin Liu
llx0129@i.smu.edu.cn
Xiaolong Liu
lxl1979@i.smu.edu.cn
Qingling Zhang
zhangqingling@gdph.org.cn

Introduction

Colorectal cancer (CRC) ranks as the third most common type of cancer worldwide, and liver metastasis serves as the key factor driving tumor progression [1]. Liver metastases exhibit a significant level of angiogenesis and abnormal blood vessel formation [2, 3]. In recent decades, anti-angiogenic therapy has been suggested for the treatment of metastatic CRC [4]. However, a limited range of efficacy markers is available to identify patients who are prone to positively respond to anti-angiogenic therapy [5].

Extracellular vesicles (EVs) known as exosomes ranging from 30 to 150 nm in size, are abundant in proteins, miRNAs, and DNA. Increasing evidence has revealed that cancer cell-secreted exosomes play a pivotal role in tumor progression, tumor immunity, resistance to chemotherapy, and angiogenesis [6, 7]. Recently, it has been reported that miRNAs serve as vital mediators of the cancer-stroma crosstalk [8, 9]. Cancer-secreted exosomal miRNAs have the potential to be transferred to normal host cells, thereby regulating target genes and mediating the progression of various tumors [10, 11]. Moreover, exosomes derived from the serum of cancer patients have been validated to be reliable diagnostic markers, with miRNAs within exosomes demonstrating greater stability than free miRNAs in serum [12–15]. Previous studies have found that miR-1825 was upregulated and related to poor prognoses in hepatocellular carcinoma [16], prostate cancer [17], and CRC [18]. But it wasn't known whether miR-1825 existed in exosomes or not in CRC. Through bioinformatics analysis, we identified that miR-1825 was significantly elevated in the serum exosome of CRC patients. Nevertheless, the function and mechanism of exosome miR-1825 in CRC remain unclear.

In this study, we demonstrated that miR-1825 was associated with CRC angiogenesis. Based on a series of in vitro and in vivo experiments, CRC-secreted exosomal miR-1825 stimulates vascular endothelial cell proliferation by targeting ING1 and activating the TGF-β/Smad2/Smad3 signaling pathway, thereby promoting angiogenesis. Therefore, our data suggest that exosomal miR-1825 may be a promising therapeutic target for colorectal cancer angiogenesis.

Results

MiR-1825 expression positively correlates with microvascular density in CRC

To screen potentially high levels of circulating exosomal miRNAs in CRC, we analyzed miRNA data from the GSE39833 database, profiled from serum exosomes in healthy controls and CRC patients by array. Within the database, miR-1825 and miR-654-5p were markedly upregulated in CRC patients, which had not been reported previously (Fig. 1A and Figure. S1A-C). We then performed RT-PCR analysis in 10 cases of CRC, and the result identified that miR-1825, but not miR-654-5p, was significantly upregulated (Fig. 1B and Figure. S1D). Compared to the low expression of miR-1825 in normal colorectal tissues, in situ hybridization (ISH) staining in 50 cases of CRC revealed that miR-1825 was significantly high expression in CRC tissues (Fig. 1D). Moreover, miR-1825 expression was also higher in cancer-adjacent vessels than normal mucosa-adjacent vessels, and the expression of miR-1825 in CRC cells positively correlated with an increase in peritumoral microvascular density (MVD) (Fig. 1C, E). These in vivo data showed that miR-1825 was upregulated in CRC patients and suggested a positive relationship with CRC angiogenesis.

CRC-secreted miR-1825 could transfer to endothelial cells via exosomes

Based on the positive correlation between miR-1825 expression and MVD in clinical samples, we speculated whether miR-1825 could transfer from CRC cells to endothelial cells via exosomes and stimulate the increase of MVD. Using transmission electron microscopy (TEM), we identified exosomes extracted from CRC cells as cup-shaped double-sided structures (30 to 150 nm) (Fig. 2A). These extracts then were proven to be exosome, after exosome markers, CD63 and TSG101, were detected by western bolt (Fig. 2B). To further investigate the function of exosomal miR-1825, the endogenous expression of miR-1825 was analyzed in four CRC cell lines and HUVECs. RT-PCR results showed that miR-1825 was upregulated in CRC cell lines compared with HUVECs. And the expression of miR-1825 in exosomes was consistent with the expression in CRC cells (Fig. 2C). Moreover, overexpression or knockdown of miR-1825 in CRC cells resulted in the upregulation or downregulation of exosomal miR-1825 respectively (Fig. 2D). These in vitro experiments supported our hypothesis that miR-1825 was increased in CRC and could be secreted as exosomal miR-1825.

To confirm whether CRC-secreted miR-1825 could be transferred to HUVECs via exosomes, PKH67-labeled exosomes were co-cultured for 48h with HUVECs. In miR-1825 overexpression exosome groups, PKH67 dye entered the incubated HUVECs, but in the control exosome groups, PKH67 dye had not or few entered the incubated HUVECs. It indicated that the miR-1825 was specifically delivered into HUVECs (Fig. 2E). In addition, RT-PCR results showed that miR-1825 expression in HUVECs was time-dependently and dosage-dependently increasing as co-cultured with exosomal miR-1825, but no changed in the control cells (Fig. 2F, G). Taken together, these results suggested that CRC-secreted

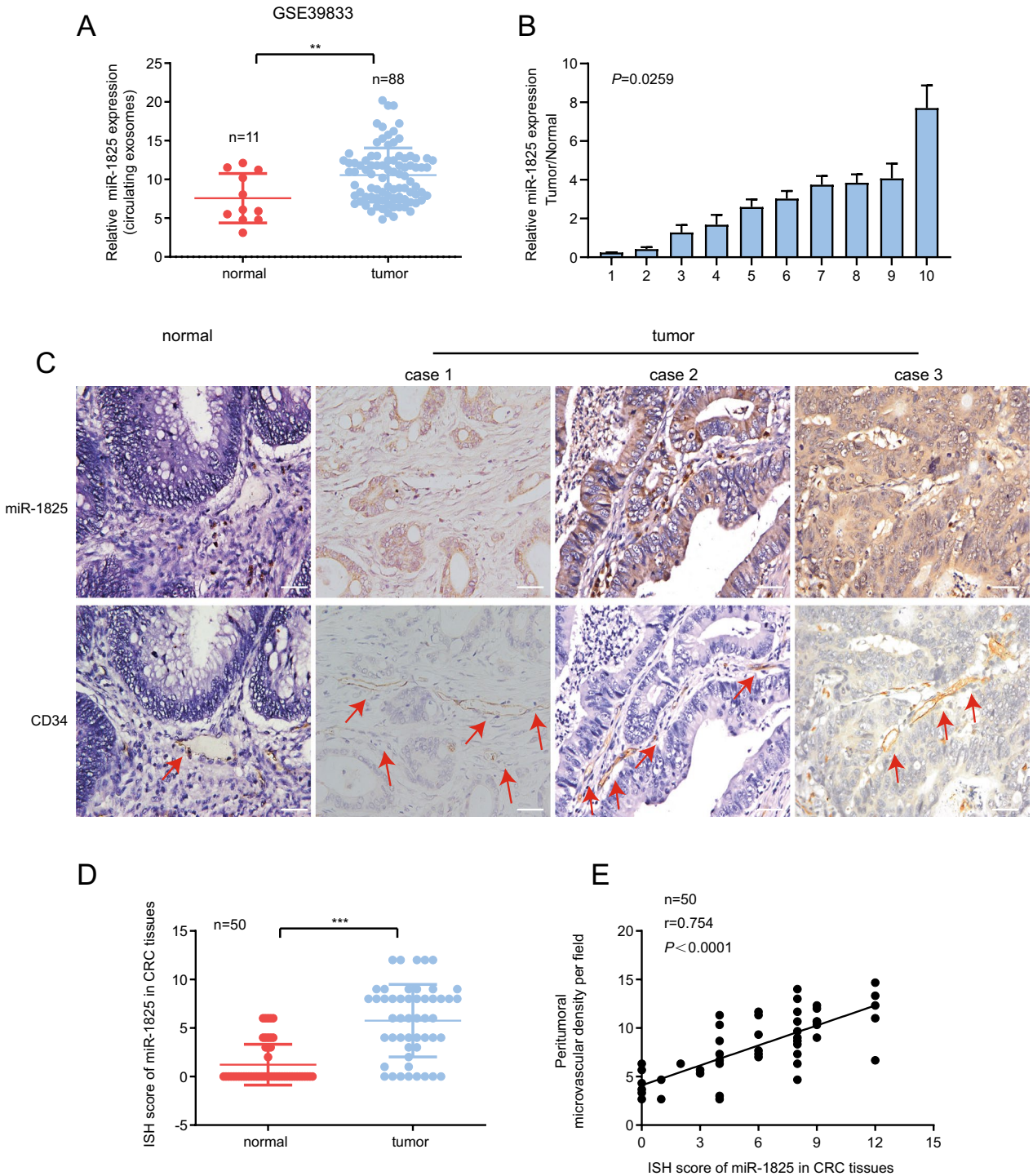

Fig. 1 miR-1825 expression positively correlates with microvascular density in CRC. **A** Relative RNA level of miR-1825 in circulating exosomes from 11 healthy donor or 88 CRC patients in GSE39833 dataset, $^{**}P < 0.01$, two-tailed Student's t-test. **B** Relative RNA level of miR-1825 in 10 CRC tissues and paired adjacent normal tissues, as determined by RT-PCR. Relative expression levels were normalized to U6. **C** Staining of miR-1825 and CD34 in serial sections of CRC specimens. Representative cases with normal tissue and CRC tissue of miR-1825 that were correspondingly stained CD34 are shown (magnification 400×). The vessels are indicated by red arrows. Scale bars, 20 μm. **D** ISH scores of miR-1825 were analyzed in 50 normal colorectal mucosa and paired CRC tissues. **E** The correlation between miR-1825 expression and microvascular density was statistically analysed by Pearson correlation coefficient

miR-1825 could be transferred to HUVECs through exosomes.

CRC-secreted exosomal miR-1825 promotes angiogenesis in vitro and in vivo

To investigate the impact of exosomal miR-1825 on endothelial cells, the migration and angiogenesis of HUVECs were examined by transwell assay, wound healing assay, tube formation assay, and aortic ring assay. Transwell assay and wound healing assay showed that co-cultured with RKO.miR-1825m-exo significantly promoted migration of HUVECs. In contrast, co-cultured with HCT116.miR-1825i-exo dramatically inhibited the migration of HUVECs (Fig. 3A–D). Tube formation assays and aortic ring assays were then performed to determine whether exosomal miR-1825 regulates angiogenesis. Compared to the control groups, co-culture with RKO.miR-1825m-exo markedly promoted angiogenesis; co-culture with HCT116.miR-1825i-exo significantly inhibited angiogenesis (Fig. 3E–H). These results suggested that exosomal miR-1825 significantly promoted angiogenesis in vitro.

The intrasplenic injection model, also known as the hepatic metastasis model, allows for reproducible and controllable induction of liver metastasis in mice, enabling the study of the metastatic microenvironment. To further investigate whether exosomal miR-1825 could regulate angiogenesis in vivo, we first established an intrasplenic injection CRC model and subsequently injected exosomes intraperitoneally weekly to assess the function of exosomal miR-1825 (Fig. 3I). We found that the administration of exosomal miR-1825 significantly promoted tumor metastasis. The liver metastatic nodules were significantly increased in the RKO.miR-1825m-exo group compared to the RKO.NCm-exo group. On the contrary, fewer liver metastatic nodules occurred in the HCT116.miR-1825i-exo group (Fig. 3J, L). Consistently, the MVD was higher in the RKO.miR-1825m-exo group than that in NCm-exo group. Compared with the control, HCT116.miR-1825i-exo treatment markedly inhibited angiogenesis in vivo (Fig. 3K, M). Collectively, these results indicated that CRC-secreted exosomal miR-1825 dramatically increased blood vessel formation and promoted tumor metastasis.

MiR-1825 targets ING1 in HUVECs

To explore how miR-1825 regulates CRC tumor angiogenesis, three miRNA databases (Targetscan, miRWalk, and miRDIP) were utilized to predict the target interaction genes of miR-1825. And screened out that ING1 was the target gene of miR-1825 among the three databases (Figure. S3A). As the members of the ING (inhibitor of growth) family, ING3 and ING4 were reported as the negative regulator of angiogenesis [19, 20]. To analyze if miR-1825 promoted angiogenesis was related to ING1, the miR-1825 binding site in the 3′ UTR of ING1 (wild type) or the mutated sequence (mutant type) was cloned into luciferase reporter plasmids (Fig. 4A) and expressed in HUVECs to assessed their response to miR-1825. It showed that miR-1825 significantly suppressed the luciferase activity of ING1 3′UTR in the ING1-WT group, but hadn't affected in the ING1-MUT group (Fig. 4B). Moreover, overexpression of miR-1825 suppressed the expression of ING1; but knocking down miR-1825 resulted in upregulation of ING1 in HUVECs (Fig. 4C–E and Figure. S3B). Then the ING1 expression level in HUVECs was assessed with the incubation of CRC-secreted exosomes (RKO.miR-1825m-exo). The IF and western blot results demonstrated that the expression of ING1 was decreased by RKO.miR-1825m-exo, but not RKO.NCm-exo. In contrast, HCT116.miR-1825i-exo dramatically increased the expression levels of ING1, indicating that ING1 in HUVECs can be mediated by exosomal miR-1825 derived from CRC cells (Fig. 4F, G). In addition, DIANA TOOLS analysis showed that high miR-1825 expression was associated with the TGF-β signaling pathway (Figure. S3C). It has been reported that activation of the TGF-β/Smad2/3 signaling pathway enhanced tumor angiogenesis [21]. The Western blot analysis revealed that incubation with RKO.miR-1825m-exo markedly increased the expressions of TGF-β, p-Smad2 and p-Smad3 in HUVECs, while incubated with HCT116.miR-1825i-exo had the opposite effect (Fig. 4G). In addition, the expressions of TGF-β, p-Smad2 and p-Smad3 were increased in RKO.miR-1825m-exo

(See figure on next page.)

Fig. 2 CRC-secreted miR-1825 is transferred to endothelial cells via exosomes. **A** Transmission electron microscopy of exosomes derived from RKO and HCT116. Scale bars, 100 nm. **B** The exosome-specific markers TSG101 and CD63 of CRC-secreted exosomes were detected by western blot. **C** RT-PCR analyzes basic expression of miR-1825 in HUVECs, CRC cell lines and paired exosomes. **D** RT-PCR analyzes relative expression of miR-1825 in indicated cell lines and paired exosomes. **E** HUVECs pre-treated with PKH67-labeled exosomes derived from the indicated cell lines were stained with phalloidin (red) and DAPI (blue) for confocal microscopy analysis. Scale bars, 20 μm. **F** RT-PCR analyzes relative expression of miR-1825 in HUVECs incubated with exosomes derived from RKO.NCm and RKO.miR-1825m for 5 ug, 10 ug, and 15 ug. **G** RT-PCR analyzes relative expression of miR-1825 in HUVECs incubated with exosomes derived from RKO.NCm and RKO.miR-1825m for 3 h, 6 h, 24 h, 36 h, and 48 h. $^{*}P < 0.05$, $^{**}P < 0.01$, $^{***}P < 0.001$, means ± SD, two-tailed Student's t-test

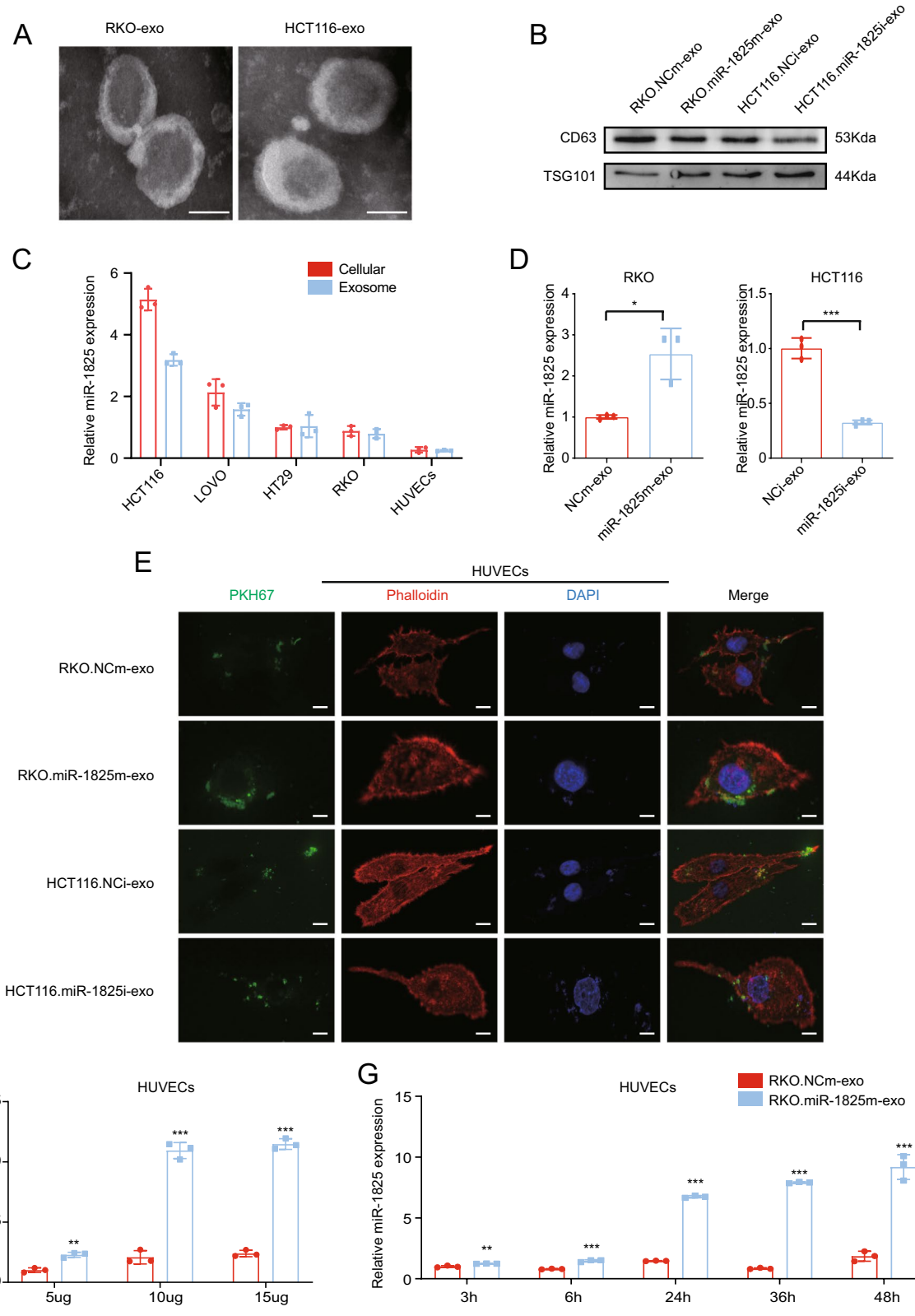

Fig. 2 (See legend on previous page.)

incubation groups, while these changes were significantly suppressed by overexpressing of ING1 (Fig. 4H). These results indicated that miR-1825 could activate the TGF-β signaling pathway via targeting ING1.

Exosomal miR-1825 promotes angiogenesis by regulating ING1

Rescue experiments were performed to investigate whether exosomal miR-1825 promoted angiogenesis by downregulating ING1. Transwell and wound healing assays showed that exosomal miR-1825 significantly promoted the migration of HUVECs in vitro, whereas restoration of ING1 expression abrogated these effects (Fig. 5A–D). Furthermore, ING1 overexpression abolished the exosomal miR-1825-induced angiogenesis (Fig. 5E–H). The relationship of miR-1825 with ING1 was further verified in vivo. It demonstrated that miR-1825 could negatively regulate ING1 expression in portal vein endothelial cells (Fig. 5I, J). These results indicated that CRC-secreted exosomal miR-1825 induces liver angiogenesis through targeting ING1.

Discussion

Exosomal miRNAs play a crucial role in mediating intercellular crosstalk, which regulate tumor immunity, invasion, and metastasis [10]. For example, exosomal miR-142-5p remodels lymphatic vessels and induces IDO to promote immune privilege in advanced cervical squamous cell carcinoma [9]. Besides, CRC-derived exosomal miR-934 is capable of inducing macrophage M2 polarization by downregulating PTEN expression, thereby promoting liver metastasis [22]. Recently, circulating exosome miRNAs have been recognized as novel non-invasive biomarkers for cancer diagnosis and prognostic evaluation. Collectively, these studies indicate that exosomal miRNAs play an important role in regulating cancer progression. In the GSE39833 cohort, we found that circulating exosomal miR-1825 levels were higher in CRC patients than in healthy donors.

Excessive angiogenesis in malignancy refers to the sprouting of new blood vessels from the vascular network formed by tumors. This process plays a crucial role in tumor proliferation, metastasis, and chemoresistance [23, 24]. Currently, angiogenesis has proven to be a prognostic indicator of the tumor and an effective therapeutic target for CRC [25, 26]. However, the effectiveness of numerous angiogenesis inhibitors needs improvement, primarily due to incomplete understanding of tumor angiogenesis. Consequently, the investigation of potential angiogenesis factors involved in tumor angiogenesis is essential, as it could serve as a new diagnostic and therapeutic target for CRC metastasis. In this study, we found that miR-1825 was significantly upregulated in CRC specimens and serum. Pruseth et al. [18] also observed a similar phenomenon. Correspondingly, miR-1825 expression was positively correlated with the increase in MVD. In addition, exosomal miR-1825 has the ability to be transferred to endothelial cells, inducing angiogenesis, and consequently promoting CRC metastasis. This suggests that exosomal miR-1825 may be a potential angiogenesis factor in tumor angiogenesis.

Previous studies have found that miR-1825 is involved in amyotrophic lateral sclerosis [27], cardiac regeneration [28], and cancer progression. However, the role of miR-1825 in tumorigenesis and tumor angiogenesis has not been reported. Interestingly, Our ISH and IHC results showed the level of miR-1825 in CRC cells was positively correlated with the level of miR-1825 in adjacent endothelial cells. Based on this, we proposed that exosomal miR-1825 could be transferred from CRC cells to endothelial cells. Consistently, we observed PKH67 fluorescence in HUVECs incubated with PKH67-labeled exosomes from CRC. Tumor angiogenesis exhibits distinct structural and functional characteristics compared to normal vasculature. It is characterized by structural disorder, tortuosity, uneven thickness, and excessive branching. These features could promote tumor metastasis [29]. CRC-induced angiogenesis plays a pivotal role in liver metastasis [2, 3]. In our study, the migration and tube formation abilities of endothelial cells were significantly enhanced after treatment with CRC-derived exosomal miR-1825. Furthermore, in vivo assays demonstrated that CRC-secreted exosomal miR-1825 dramatically increased blood vessel formation and promoted liver metastasis. These results indicated that exosomal miR-1825

(See figure on next page.)

Fig. 3 CRC-secreted exosomal miR-1825 promotes angiogenesis in vitro and in vivo. **A**, **B** Transwell assays analyze the migration of co-cultured HUVECs in each group. Scale bars, 100 μm. **C**, **D** Wound healing assays analyze the migration of co-cultured HUVECs in each group. Scale bars, 100 μm. **E**, **F** Tube formation assays analyze the angiogenesis of co-cultured HUVECs in each group. Scale bars, 50 μm. **G**, **H** Aortic ring assays analyze the angiogenesis of co-cultured HUVECs in each group. Scale bars, 200 μm. **I** Schematic diagram of hepatic metastasis experiments in nude mice. **J**, **L** Gross and H&E staining observe the liver metastasis in each group. The liver metastasis nodules are indicated by red arrows. Means ± SD are provided (n = 5). The scale bar at 100 × magnification represents 50 μm. The scale bar at 400 × magnification represents 20 μm. **K**, **M** IHC staining for CD34 quantitatively assesses for angiogenesis in each group. Scale bars, 20 μm. *$P < 0.05$, **$P < 0.01$, ***$P < 0.001$, means ± SD, two-tailed Student's t-test

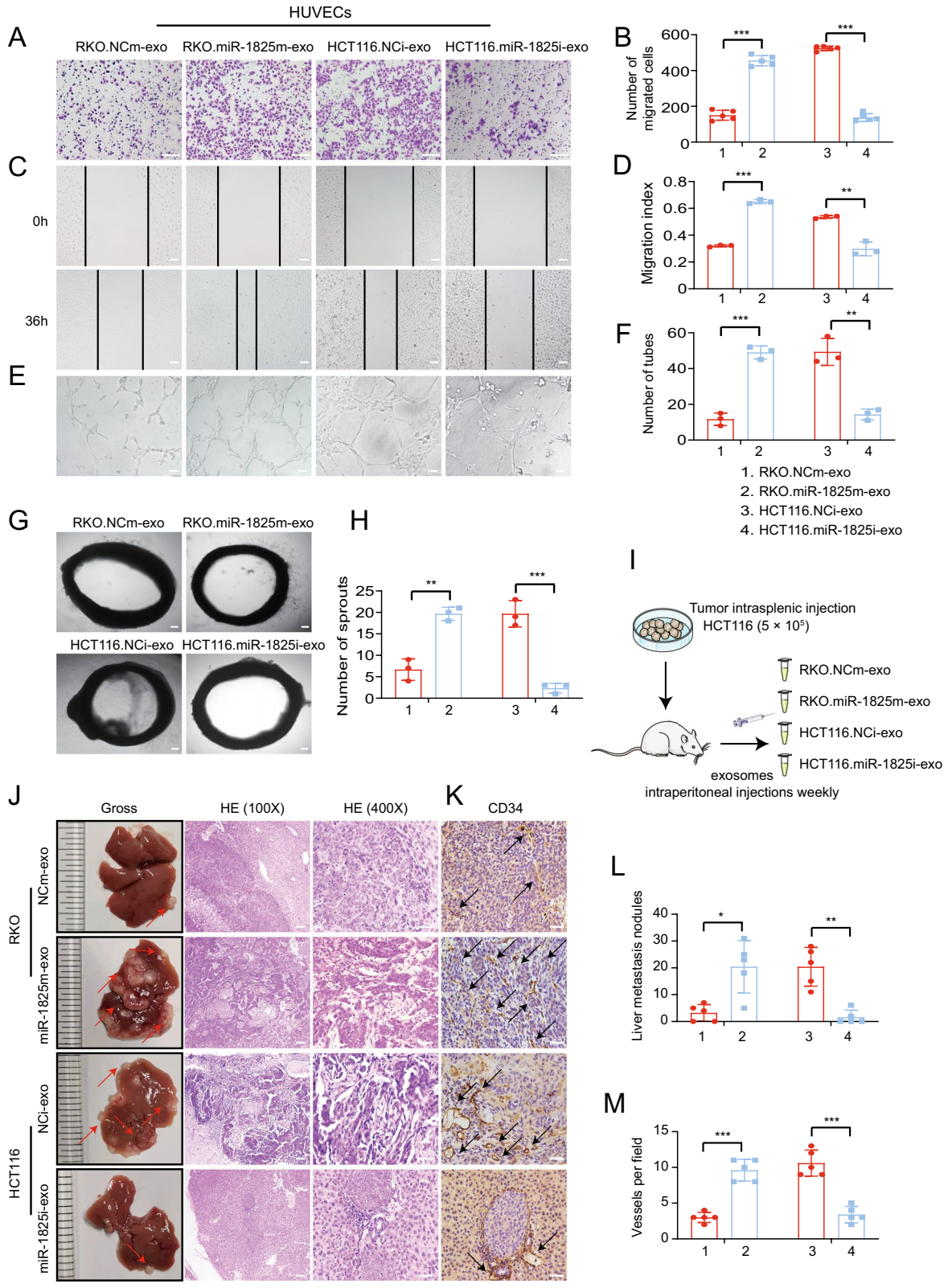

Fig. 3 (See legend on previous page.)

promotes CRC-induced angiogenesis and contributes to CRC metastasis.

The inhibitor of growth (ING) family members (ING1-5), as tumor suppressors, are crucial regulators of cell growth and proliferation, cell cycle checkpoints, apoptosis, and cellular senescence [30]. Overexpression of the nuclear localization sequence KKFK of ING3 inhibits angiogenesis of melanoma cells [20]. ING4 is considered an angiogenesis suppressor in a variety of solid tumors. ING4 can physically interact with the p65 (RelA) to regulate the expression of the angiogenesis-related gene IL-8, thereby inhibiting brain tumor angiogenesis [19]. In addition, JFK-mediated ING4 ubiquitination and degradation lead to the hyperactivation of the NF-κB pathway, which leads to angiogenesis and metastasis in breast cancer [31]. ING1 has been reported to function as a tumor suppressor in breast cancer [32], lung cancer [33], colorectal cancer [34], and gastric cancer [35]. The loss of ING1 is also associated with the tumorigenesis of B-cell lymphoma and soft tissue sarcoma [36]. Using three miRNA databases, ING1 was screened as a possible target gene of miR-1825 to regulate angiogenesis. In this study, our data identified that miR-1825 in endothelial cells downregulates ING1 and ING1 as a direct target of miR-1825. Moreover, exosomal miR-1825 from CRC cells promoted angiogenesis and tumor metastasis by silencing ING1. In addition, bioinformatics analysis revealed a noteworthy connection between miR-1825 and TGF-β/Smad2/3 signaling pathway. And previous studies have noted the pro-angiogenic properties of the TGF-β/Smad2/Smad3 pathway in vascular endothelial cells [37, 38]. In our study, we found that HUVECs treated with high miR-1825 level exosomes activated the TGF-β/Smad2/Smad3 signaling pathway. In contrast, restoration of ING1 expression in exosomes-treated HUVECs abolished these effects. Collectively, these results validated that exosomal miR-1825 induces CRC angiogenesis by targeting ING1 to activate TGF-β/Smad2/Smad3 (Fig. 6).

Conclusion

In summary, our study demonstrated the important role of exosomal miR-1825 in regulating CRC angiogenesis. We found that miR-1825 was highly expressed in paracancerous blood vessels and positively correlated with MVD. The CRC-secreted exosomal miR-1825 could be transferred to vascular endothelial cells, subsequently inhibiting ING1 and activating the TGF-β/Smad2/Smad3 signaling pathway, thereby promoting angiogenesis and liver metastasis of CRC (Fig. 6). This new finding identified the intercellular miR-1825-ING1 axis as a key molecular mechanism of CRC progression and may serve as a potential diagnostic and therapeutic target for CRC patients.

Materials and methods

Clinical specimens

50 Paraffin-embedded CRC specimens and 10 fresh CRC tissues were collected from patients who underwent surgical treatment without prior radiotherapy and chemotherapy in the Third Affiliated Hospital of Southern Medical University. The study received approval by the Ethical Committee of the Third Affiliated Hospital of Southern Medical University (ID number 2021-038). Informed consent was obtained from each patient prior to sample collection.

Cell culture

Human CRC cell lines HCT116, LOVO, RKO and HT29, and human umbilical vein endothelial cells (HUVECs) were purchased from the American Type Culture Collection (ATCC). HCT116, LOVO, RKO and HT29 were cultured in PPMI-1640 medium containing 10% fetal bovine serum (Thermo Scientific, Waltham, MA, United States). HUVECs was cultured in F12-K medium supplemented with 10% fetal bovine serum.

Exosomes isolation, characterization, and treatment

The fetal bovine serum underwent overnight centrifugation at 120,000 g at 4 °C to remove exosomes. CRC cells were cultured in PPMI-1640 medium supplemented with 10% fetal bovine serum, and supernatants were collected after 48 h. Exosomes were isolated from CRC-derived

(See figure on next page.)

Fig. 4 ING1 is a functional target of miR-1825 in HUVECs. **A** The binding regions of miR-1825, the seed recognizing sites in the ING1 3′ UTR, and the ING1 mutant sequence are shown. **B** Luciferase activities of 3′UTR ING1-luc constructs in HUVECs after transfection with miR-1825 mimics. Means ± SD are provided (n = 3). *$P < 0.05$, means ± SD, two-tailed Student's t-test. **C**, **D** HUVECs are transfected with mimics-NC, miR-1825 mimics, inhibitor-NC, and miR-1825 inhibitor. RT-PCR analyzes relative expression of miR-1825 and ING1 in indicated cell lines. **$P < 0.01$, ***$P < 0.001$, means ± SD, two-tailed Student's t-test. **E** Western blot analysis of ING1 protein in indicated cell lines. **F** Immunofluorescence staining analysis of ING1 in co-cultured HUVECs in each group. Scale bars, 10 μm. **G** Western blot analysis of ING1, TGF-β, p-Smad2, Smad2, p-Smad3 and Smad3 protein in co-cultured HUVECs in each group. **H** Western blot analysis of ING1, TGF-β, p-Smad2, Smad2, p-Smad3 and Smad3 protein in indicated cell lines

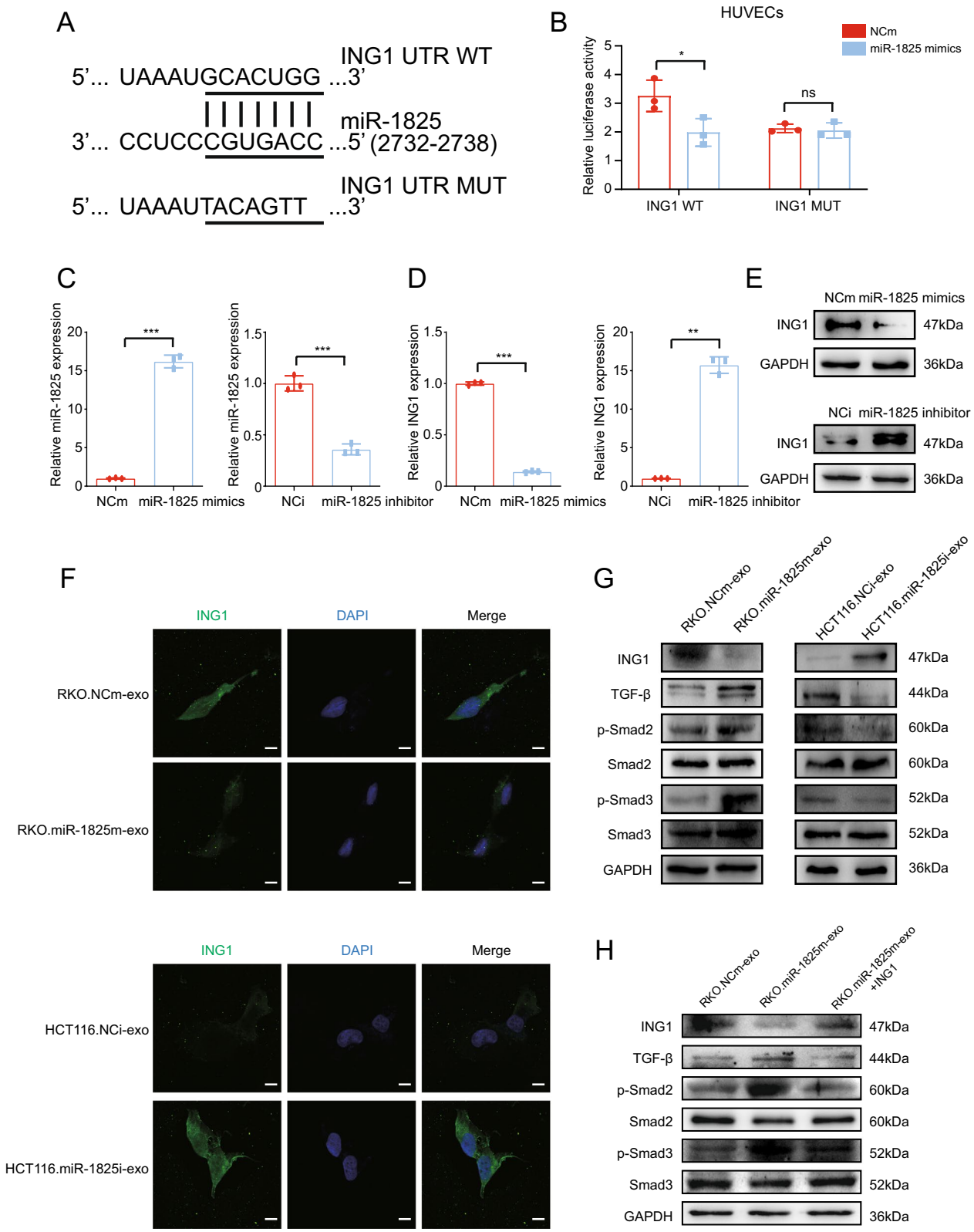

Fig. 4 (See legend on previous page.)

supernatant through ultracentrifugation at 4 °C. First, the supernatant underwent centrifugation at 500 g for 10 min to remove cells and cell debris; then, it was centrifuged at 16,800 g for 30 min. The supernatant was then filtered with a 0.22 um filter (Millipore) and ultracentrifuged at 110,000 g for 70 min. Finally, the exosome pellets were washed with PBS followed by a second ultracentrifugation at 110,000 g for 70 min and then resuspended in PBS.

For transmission electron microscopy, exosomes were fixed with 2% glutaraldehyde and placed on the copper carrier grids. The grids were then stained using 2% phosphotungstic acid and visualised by transmission electron microscopy (Hitachi H-7650). For the exosome uptake experiment, exosomes were labeled using PKH67 membrane dye (Sigma) according to the manufacturer's instructions. After incubation with labeled exosomes for 48 h, HUVECs were stained with phalloidin (Abcam). For in vitro treatment, 10 μg of exosomes were incubated with 1×10^5 HUVECs for 48 h.

Cell transfection

Lentivirus vectors expressing miR-1825 and repressing miR-1825 were constructed and generated by Genechem (Shanghai, China). Mimics and Inhibitor of miR-1825 were purchased from Kidan Biosciences co. The 3′ UTR wild-type or mutated ING1-luc plasmid and ING1 expressing plasmid were constructed and generated by Genechem (Shanghai, China). The sequences of all indicated lentivirus were listed in supplementary Table 1.

In situ hybridization (ISH) and Immunohistochemistry (IHC)

The miR-1825 detection probe was purchased from Kidan Biosciences co. ISH was performed in tissue sections using ISH kit (Boster Co, Wuhan, China) by following the manufacturer's instructions. ISH assay was performed under RNase-free conditions.

Paraffin-embedded tissues were dewaxed from xylene, rehydrated in a graded ethanol series to water. Then, sections were immersed in 3% hydrogen peroxide for 10 min and incubated with primary antibody CD34 (1:200 dilution, Abcam) overnight at 4 °C. Subsequently, corresponding secondary antibodies were applied and incubated for 1 h at room temperature. Targeted molecules were visualized by using DAB and counterstained with hematoxylin. These results were scored as previously described as the total of the staining intensity and percentage of positive tumor cells [39].

Immunofluorescence

Immunofluorescence of cells was performed according to the previous study [40]. Immunofluorescence images were captured by confocal microscopy (Zeiss LSM 900). The following primary antibodies were used: ING1 (1:150 dilution, R&D Systems).

Quantitative reverse transcription PCR (RT-PCR)

Total RNA was extracted from tissues, cells lines and exosomes by using Trizol (TAKARA, Dalian, China) according to the manufacturer's instructions. Reverse transcription was performed using the Mir-X™ miRNA First-Strand Synthesis Kit (TaKaRa) for miRNAs or PrimeScript™ RT Master Mix (TaKaRa) for genes. RT-PCR was conducted using SYBR Green PCR Master Mix (TaKaRa) and performed on Applied Biosystems 7500 Sequence Detection system (Applied Biosystems). The sequences of all indicated primers were listed in supplementary Table 2.

Western blotting

Cells or exosomes were lysed in RIPA buffer and quantified using Bradford Protein Assay (KeyGEN BioTECH, China). Subsequently, the lysates were subjected to SDS–PAGE, transferred onto the PVDF membranes (Millipore). Then membranes were blocked with 5% BSA in PBST buffer and incubated with primary antibodies overnight at 4 °C. The following primary antibodies were used: CD63 (1:1000 dilution, ABclonal, Cat# A5271), TSG101 (1:1000 dilution, Immunoway, Cat# YT4760), ING1 (1:1000 dilution, ABclonal, Cat# A7904), TGF-β (1:1000 dilution, Affinity, Cat# AF1027), Smad2 (1:1000 dilution, Cell Signaling Technology, Cat# 5339), p-Smad2 (1:1000 dilution, Cell Signaling Technology, Cat# 18338), Smad3 (1:1000 dilution, Cell Signaling Technology, Cat# 9513), p-Smad3 (1:1000 dilution, Cell Signaling Technology, Cat# 9520), GAPDH (1:2000, Proteintech, Cat# 10494-1-AP).

(See figure on next page.)

Fig. 5 Exosomal miR-1825 promotes angiogenesis by regulating ING1. HUVECs pre-treated with exosomes derived from RKO.miR-1825m were transfected with ING1 plasmid. **A**, **B** Transwell assays analyze the migration of indicated cell lines. Scale bars, 100 μm. **C**, **D** Wound healing assays analyze the migration of indicated cell lines. Scale bars, 100 μm. **E**, **F** Tube formation assays analyze the angiogenesis of indicated cell lines. Scale bars, 50 μm. **G**, **H** Aortic ring assays analyze the angiogenesis of indicated cell lines. Scale bars, 200 μm. $^{**}P<0.01$, $^{***}P<0.001$, means ± SD, two-tailed Student's t-test. **I**, **J** Immunofluorescence staining analysis of ING1 expression (red) in hepatic vessels in each group. The vascular structures were labeled by CD34 (green). Scale bars, 20 μm

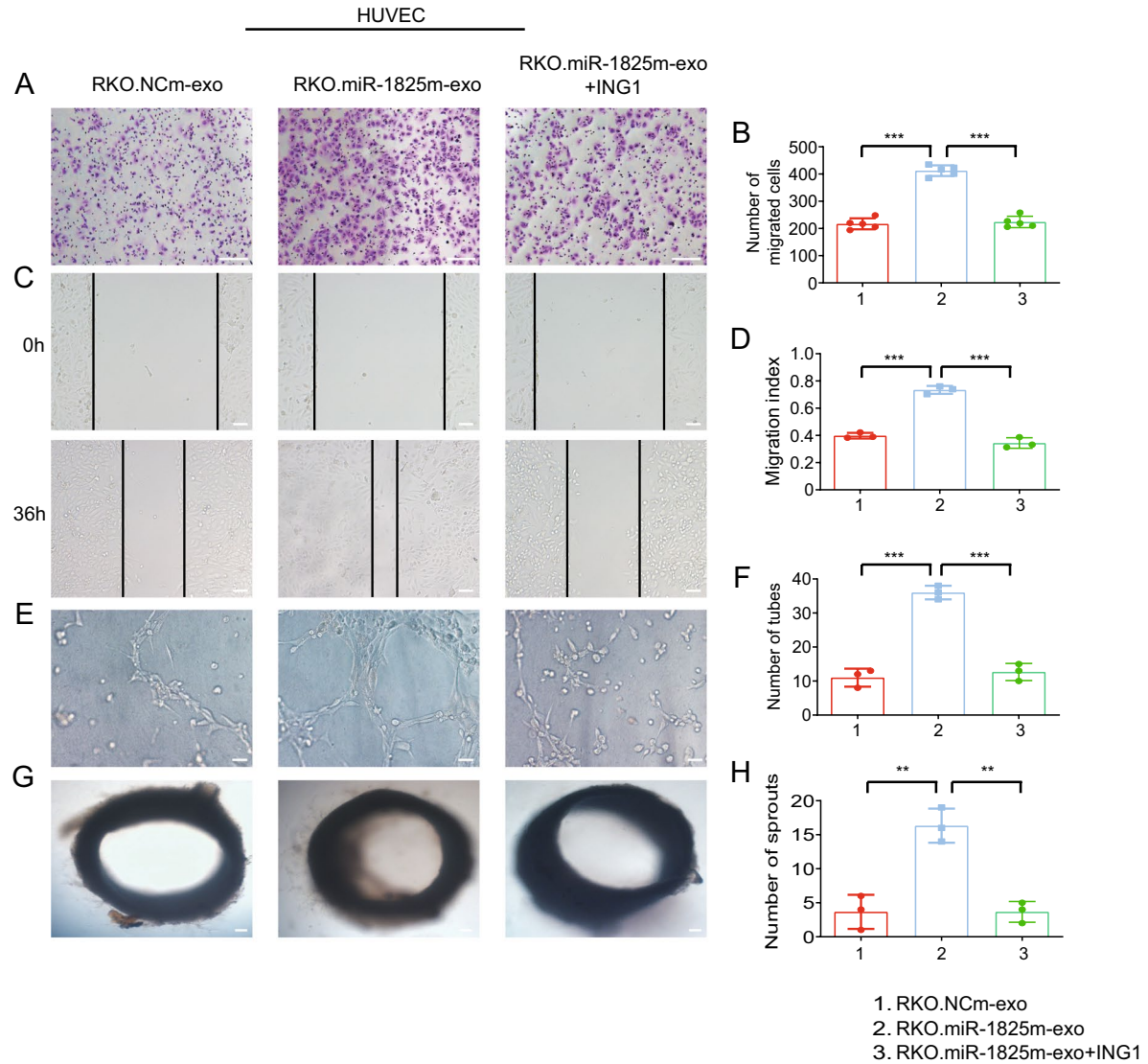

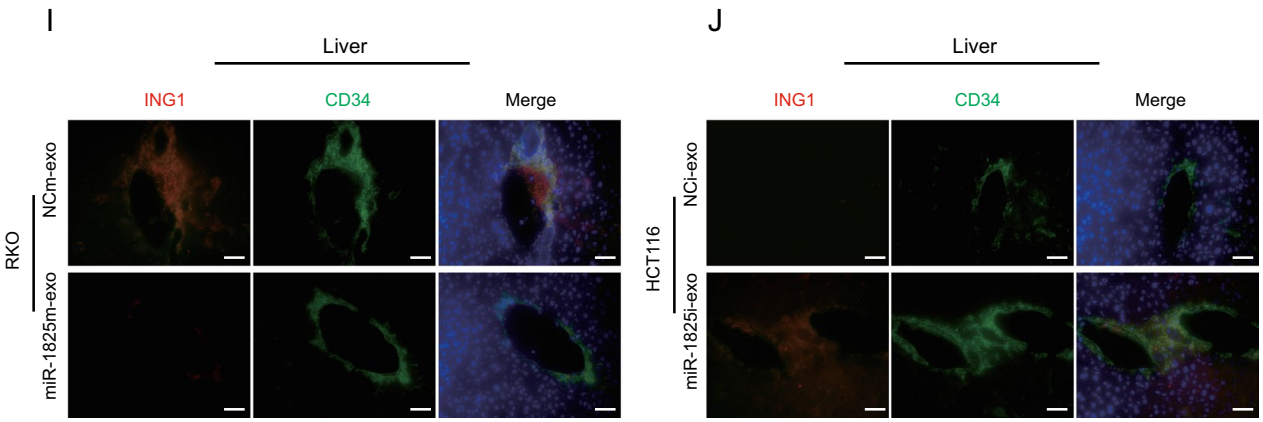

Fig. 5 (See legend on previous page.)

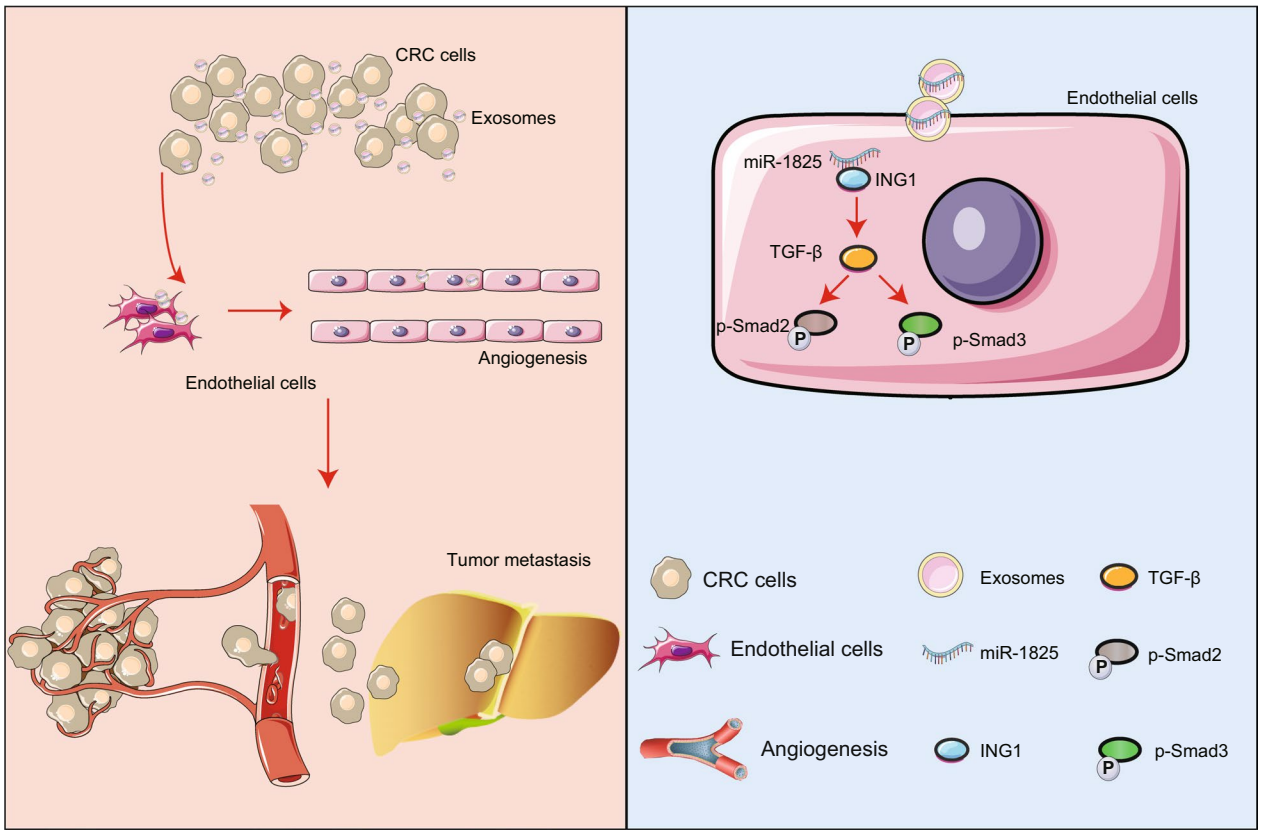

Fig. 6 Schematic diagram showing the mechanism whereby CRC-secreted miR-1825 promotes angiogenesis by downregulating ING1 and activating the TGF-β/Smad2/Smad3 signaling pathway

Finally, the membranes were incubated with secondary antibody and developed with ECL substrate and imaged using the enhanced chemiluminescence detection system (Tennon5200, China).

Migration assay and wound healing assay

For transwell migration assay, cell suspensions (1×10^5 cells of the exosomes-treated HUVECs) were diluted into 200 µl of serum-free medium and added to the upper transwell chambers (BD Biosciences, CA, USA) and the medium containing 10% FBS was placed into the bottom chamber. After 12 h, migrated cells on the undersides of the membranes were stained with crystal violet and counted in five fields (100×) for further statistical analysis.

For wound healing assays, the exosomes-treated HUVECs were seeded into 12-well plates and scratched with a pipette tip after 24 h. Images were observed at the indicated times, and wound width at 36 h relative to 0 h was evaluated to assess wound healing. Experiments were repeated three times.

Tube formation assay and aortic ring assay

For tube formation assay, matrigel matrix (Corning) was placed in µ–SlideAngiogenesis (ibidi), and exosomes-treated HUVECs (1×10^4 cells) were seeded in the coated wells. After incubation at 37 °C for 12 h, tube formation was observed with a microscope (200×). The ability of tube formation was determined by measuring the number of tubes. Aortic ring assay was performed as described in our previous study [40].

Animal models

20 four-to-six-week-old male BALB/c nude mice (nu/nu) were purchased from Guangdong Medical Laboratory Animal Center (Guangdong, China) and treated according to the Animal Research Reporting of In vivo Experiments (ARRIVE) guidelines. Mice were anesthetized and exposed the spleen by the laparotomy. 5×10^5 cells of HCT116 were suspended in 100 µl of PBS and injected into the distal part of the spleen with an insulin syringe. 20 mice were randomly divided into four groups for further experiments, and 10 µg of exosomes from overexpression or knockdown of miR-1825 CRC

cells resuspended in 50 µl of PBS were injected intraperitoneally weekly. After 4 weeks, the mice were sacrificed, and the livers were collected for further analysis.

Dual-luciferase reporter system analysis

The wild-type or mutated 3'-UTR of ING1 gene were inserted into the luciferase vector. HUVECs was cotransfected with the vectors and miR-1825, which were subsequently harvested and analyzed for luciferase activity by the Luc-pair™ Duo-Luciferase HS assay kit (GeneCopoeia, China). Three independent experiments were performed.

Statistical analysis

Each experiment was performed at least three times. Statistical analyses were performed using Prism 8.0 (La Jolla, CA, USA). Student's t-test and one-way analysis of variance (ANOVA) were used to evaluate the significance of the differences among different groups. The correlation analysis was detected by Pearson's correlation coefficient. All data were presented as the means ± standard deviation (SD).

Supplementary Information

The online version contains supplementary material available at https://doi.org/10.1186/s12935-025-03674-5.

Supplementary material 1.

Author contributions

JS, JL and JL carried out the experiments. JS, JL and JL contributed equally to this work. JS, YL and YX participated in data analysis and animal experiments. HW, LL and XL gave assisted in collecting tissue samples. QZ and JS designed the study and wrote the manuscript. All authors read and approved the final manuscript.

Funding

This project was supported by grants of Key R&D Program Projects in Guangdong Province (QI. Z, 2021B0101420005); the National Natural Science Foundation of China (QI. Z, 8197227 and 82173033; YW. X, 82102712); China Postdoctoral Science Foundation (YW. X, 2021M690751); High-level Hospital Construction Project (QI. Z, DFJHBF202108 and YKY-KF202204); Guangdong Provincial Key Laboratory of Artificial Intelligence in Medical Image Analysis and Application (QI. Z, No. 2022B1212010011); Guangdong Basic and Applied Basic Research Foundation (XL. L, 2022A1515012290); Guangzhou Science & Technology Project (LX.L 202201011772, and JB. S, 2024A04J4807); President Foundation of The Third Affiliated Hospital of Southern Medical University (XL. L, YM202208, YP202217 and JB. S, YQ202214).

Data availability

No datasets were generated or analysed during the current study.

Declarations

Ethics approval and consent to participate

Informed consent was obtained to bank CRC tissues for research purposes. The collection of CRC tissues for research purposes was approved by the Ethics Committee of the Third Affiliated Hospital of Southern Medical University. All protocols for animal studies were reviewed and approved by the Institutional Animal Care and Use Committee of Southern Medical University.

Competing interests

The authors declare no competing interests.

Author details

[1]Department of Pathology, Guangdong Provincial People's Hospital (Guangdong Academy of Medical Sciences), Southern Medical University, Guangzhou 510080, Guangdong, China. [2]Department of General Surgery, The Third Affiliated Hospital of Southern Medical University, 183 West Zhongshan Avenue, Guangzhou 510630, Guangdong, People's Republic of China.

Received: 12 October 2024 Accepted: 4 February 2025
Published online: 22 February 2025

References

1. Siegel RL, Miller KD, Fuchs HE, Jemal A. Cancer statistics, 2022. CA Cancer J Clin. 2022;72:7–33. https://doi.org/10.3322/caac.21708.
2. Xu B, Shen F, Cao J, Jia L. Angiogenesis in liver metastasis of colo-rectal carcinoma. Front Biosci. 2013;18:1435–43. https://doi.org/10.2741/4190.
3. Zhu B, et al. DNMT1-induced miR-378a-3p silencing promotes angiogenesis via the NF-kappaB signaling pathway by targeting TRAF1 in hepatocellular carcinoma. J Exp Clin Cancer Res. 2021;40:352. https://doi.org/10.1186/s13046-021-02110-6.
4. Itatani Y, Kawada K, Yamamoto T, Sakai Y. Resistance to anti-angiogenic therapy in cancer-alterations to anti-VEGF pathway. Int J Mol Sci. 2018. https://doi.org/10.3390/ijms19041232.
5. Schiffmann LM, Bruns CJ, Schmidt T. Resistance mechanisms of the metastatic tumor microenvironment to anti-angiogenic therapy. Front Oncol. 2022;12:897927. https://doi.org/10.3389/fonc.2022.897927.
6. Yang E, et al. Exosome-mediated metabolic reprogramming: the emerging role in tumor microenvironment remodeling and its influence on cancer progression. Signal Transduct Target Ther. 2020;5:242. https://doi.org/10.1038/s41392-020-00359-5.
7. Wang SE. Extracellular vesicles in cancer therapy. Semin Cancer Biol. 2022. https://doi.org/10.1016/j.semcancer.2022.06.001.
8. He Q, et al. Cancer-secreted exosomal miR-21-5p induces angiogenesis and vascular permeability by targeting KRIT1. Cell Death Dis. 2021;12:576. https://doi.org/10.1038/s41419-021-03803-8.
9. Zhou C, et al. Exosome-derived miR-142-5p remodels lymphatic vessels and induces IDO to promote immune privilege in the tumour microenvironment. Cell Death Differ. 2021;28:715–29. https://doi.org/10.1038/s41418-020-00618-6.
10. Jia Z, Jia J, Yao L, Li Z. Crosstalk of exosomal non-coding RNAs in the tumor microenvironment: novel frontiers. Front Immunol. 2022;13:900155. https://doi.org/10.3389/fimmu.2022.900155.
11. Liu QW, He Y, Xu WW. Molecular functions and therapeutic applications of exosomal noncoding RNAs in cancer. Exp Mol Med. 2022;54:216–25. https://doi.org/10.1038/s12276-022-00744-w.
12. Melo SA, et al. Cancer exosomes perform cell-independent microRNA biogenesis and promote tumorigenesis. Cancer Cell. 2014;26:707–21. https://doi.org/10.1016/j.ccell.2014.09.005.
13. Zhou W, et al. Cancer-secreted miR-105 destroys vascular endothelial barriers to promote metastasis. Cancer Cell. 2014;25:501–15. https://doi.org/10.1016/j.ccr.2014.03.007.
14. Yu W, et al. Exosome-based liquid biopsies in cancer: opportunities and challenges. Ann Oncol. 2021;32:466–77. https://doi.org/10.1016/j.annonc.2021.01.074.
15. Hoshino A, et al. Tumour exosome integrins determine organotropic metastasis. Nature. 2015;527:329–35. https://doi.org/10.1038/nature15756.
16. Pascut D, et al. A comparative characterization of the circulating miRNome in whole blood and serum of HCC patients. Sci Rep. 2019;9:8265. https://doi.org/10.1038/s41598-019-44580-x.
17. Guo X, et al. Five microRNAs in serum as potential biomarkers for prostate cancer risk assessment and therapeutic intervention. Int Urol Nephrol. 2018;50:2193–200. https://doi.org/10.1007/s11255-018-2009-4.
18. Pruseth B, Ghosh A, Pradhan D, Purkait S, Guttula PK. Analysis of overexpressed miRNA in circulation and cancer tissue to develop a potential microRNA panel for the diagnosis of colorectal cancer. Microrna. 2021;10:250–62. https://doi.org/10.2174/2211536611666211228102644.

19. Garkavtsev I, et al. The candidate tumour suppressor protein ING4 regulates brain tumour growth and angiogenesis. Nature. 2004;428:328–32. https://doi.org/10.1038/nature02329.
20. Zhou R, et al. Nuclear localization of ING3 is required to suppress melanoma cell migration, invasion and angiogenesis. Biochem Biophys Res Commun. 2020;527:418–24. https://doi.org/10.1016/j.bbrc.2020.04.056.
21. Batlle R, et al. Regulation of tumor angiogenesis and mesenchymal-endothelial transition by p38alpha through TGF-beta and JNK signaling. Nat Commun. 2019;10:3071. https://doi.org/10.1038/s41467-019-10946-y.
22. Zhao S, et al. Tumor-derived exosomal miR-934 induces macrophage M2 polarization to promote liver metastasis of colorectal cancer. J Hematol Oncol. 2020;13:156. https://doi.org/10.1186/s13045-020-00991-2.
23. Majidpoor J, Mortezaee K. Angiogenesis as a hallmark of solid tumors - clinical perspectives. Cell Oncol (Dordr). 2021;44:715–37. https://doi.org/10.1007/s13402-021-00602-3.
24. Cho WC, Jour G, Aung PP. Role of angiogenesis in melanoma progression: Update on key angiogenic mechanisms and other associated components. Semin Cancer Biol. 2019;59:175–86. https://doi.org/10.1016/j.semcancer.2019.06.015.
25. Hansen TF, Qvortrup C, Pfeiffer P. Angiogenesis inhibitors for colorectal cancer. A review of the clinical data. Cancers. 2021. https://doi.org/10.3390/cancers13051031.
26. Wang K, Chen Q, Liu N, Zhang J, Pan X. Recent advances in, and challenges of, anti-angiogenesis agents for tumor chemotherapy based on vascular normalization. Drug Discov Today. 2021;26:2743–53. https://doi.org/10.1016/j.drudis.2021.07.024.
27. Aksu-Menges E, et al. Two distinct skeletal muscle microRNA signatures revealing the complex mechanism of sporadic ALS. Acta Neurol Belg. 2021. https://doi.org/10.1007/s13760-021-01743-w.
28. Pandey R, et al. MicroRNA-1825 induces proliferation of adult cardiomyocytes and promotes cardiac regeneration post ischemic injury. Am J Transl Res. 2017;9:3120–37.
29. Viallard C, Larrivee B. Tumor angiogenesis and vascular normalization: alternative therapeutic targets. Angiogenesis. 2017;20(4):409–26.
30. Nouman GS, Anderson JJ, Lunec J, Angus B. The role of the tumour suppressor p33 ING1b in human neoplasia. J Clin Pathol. 2003;56:491–6. https://doi.org/10.1136/jcp.56.7.491.
31. Yan R, et al. SCF(JFK) is a bona fide E3 ligase for ING4 and a potent promoter of the angiogenesis and metastasis of breast cancer. Genes Dev. 2015;29:672–85. https://doi.org/10.1101/gad.254292.114.
32. Thakur S, Nabbi A, Klimowicz A, Riabowol K. Stromal ING1 expression induces a secretory phenotype and correlates with breast cancer patient survival. Mol Cancer. 2015;14:164. https://doi.org/10.1186/s12943-015-0434-x.
33. Jiang M, Zhou LY, Xu N, An Q. Down-regulation of miR-500 and miR-628 suppress non-small cell lung cancer proliferation, migration and invasion by targeting ING1. Biomed Pharmacother. 2018;108:1628–39. https://doi.org/10.1016/j.biopha.2018.09.145.
34. Gao Z, et al. miR-24-3p promotes colon cancer progression by targeting ING1. Signal Transduct Target Ther. 2020;5:171. https://doi.org/10.1038/s41392-020-0206-y.
35. Guo XB, et al. Down-regulation of miR-622 in gastric cancer promotes cellular invasion and tumor metastasis by targeting ING1 gene. World J Gastroenterol. 2011;17:1895–902. https://doi.org/10.3748/wjg.v17.i14.1895.
36. Guerillon C, Larrieu D, Pedeux R. ING1 and ING2: multifaceted tumor suppressor genes. Cell Mol Life Sci. 2013;70:3753–72. https://doi.org/10.1007/s00018-013-1270-z.
37. Chen W, He S, Xiang D. Hypoxia-induced retinal pigment epithelium cell-derived bFGF promotes the migration and angiogenesis of HUVECs through regulating TGF-beta1/smad2/3 pathway. Gene. 2021;790:145695. https://doi.org/10.1016/j.gene.2021.145695.
38. Wu M, et al. SHED aggregate exosomes shuttled miR-26a promote angiogenesis in pulp regeneration via TGF-beta/SMAD2/3 signalling. Cell Prolif. 2021;54:e13074. https://doi.org/10.1111/cpr.13074.
39. Zhang YY, Wang QM, Niu HL, Liu X, Zhang QL. The general expression analysis of WTX gene in normal and cancer tissues. Pathol Oncol Res. 2017;23:439–46. https://doi.org/10.1007/s12253-016-0168-0.
40. Zeng Z, et al. Cancer-derived exosomal miR-25-3p promotes pre-metastatic niche formation by inducing vascular permeability and angiogenesis. Nat Commun. 2018;9:5395. https://doi.org/10.1038/s41467-018-07810-w.

Publisher's Note